Physica B 403 (2008) 3295–3301

Contents lists available at ScienceDirect

Physica B

journal homepage: www.elsevier.com/locate/physb

Room-temperature ferromagnetism in Dy films doped with Ni

I. Edelman [a,*], S. Ovchinnikov [a,b], V. Markov [a], N. Kosyrev [a], V. Seredkin [a], A. Khudjakov [a], G. Bondarenko [a], V. Kesler [c]

[a] Kirensky Institute of Physics, Siberian Division, Russian Academy of Sciences, Akademgorodok, Krasnoyarsk 660036, Russia
[b] Siberian Federal University, Av. Svobodnyi 71, Krasnoyarsk 660074, Russia
[c] Institute of Semiconductor Physics, Siberian Division, Russian Academy of Sciences, Av. Akademika Lavrent'eva 13, Novosibirsk 630090, Russia

ARTICLE INFO

Article history:
Received 30 October 2007
Received in revised form
17 April 2008
Accepted 17 April 2008

PACS:
73.20.At
73.61.At
75.70.−i

Keywords:
Dy
Dy–Ni bi-layer films
Magnetic ordering
Magnetic circular dichroism
Magneto-optic Kerr effect
Auger spectroscopy

ABSTRACT

Temperature, magnetic field and spectral dependences of magneto-optical effects (MOEs) in bi-layer films $Dy_{(1-x)}Ni_x$–Ni and $Dy_{(1-x)}(NiFe)_x$–NiFe were investigated, x changes from 0 to 0.06. Peculiar behavior of the MOEs was revealed at temperatures essentially exceeding the Curie temperature of bulk Dy which is explained by the magnetic ordering of the Dy layer containing Ni under the action of two factors: Ni impurities distributed homogeneously over the whole Dy layer and atomic contact of this layer with continues Ni layer. The mechanism of the magnetic ordering is suggested to be associated with the change of the density of states of the alloy $Dy_{(1-x)}Ni_x$ owing to hybridization with narrow peaks near the Fermi level character for Ni.

1. Introduction

Metallic Dy is of significant research interest as a material that has an extremely large magnetic moment: the effective magnetic moment of the trivalent Dy ion is equal to $10.65\mu_B$, Dy metal has a saturation magnetization at 0 K $M_s = 3000$ Gs which is much higher than iron (1720 Gs). However, at room temperature Dy is paramagnetic, since the transition to the ferromagnetic phase in bulk Dy occurs at $T_C = 85$ K. Despite the fact that the magnetic properties of Dy have frequently been discussed (see, e.g., Refs. [1,2]), new studies have been performed that lead to a better understanding of the magnetism of this metal [3]. The magnetic properties of Dy metal have been shown to change significantly upon going to small particles and thin-film nanostructures. In particular, the effect of the crystallite size and strain on the character of the phase transitions in fine-grained Dy samples have been studied in Ref. [4]. In Ref. [5], it was shown that helical structures do not arise in Dy nanoparticles embedded in an Al film. In Ref. [6], it was demonstrated that the Curie temperature T_C decreases or increases in Dy epitaxial films incorporated in Y–Dy–Y and Er–Dy–Er sandwiches, respectively, and this effect was explained in term of stretching or compression of the Dy single crystal along the c axis because of the larger Y and smaller Er lattice parameter compared to that of Dy. The magnetic state of the rare-earth (RE) layer in film structures or superlattices can be influenced by the interaction with the neighboring 3d-metal layers or inclusions of 3d-metal atoms in the RE layer. Peculiar magnetic effects were observed in the Tb/Fe [6,7], Gd/Fe [8] and Dy/Fe [9,10] multi-layers. Magnetic order was observed in very thin (1.0–1.5 nm in thickness) RE-metal layers at the boundary with 3d transition-metal layers at temperatures exceeding T_C of the corresponding RE bulk metal [11,12].

Recently, we have shown a strong influence of low Ni-impurity concentrations in Dy layers on the temperature and spectral dependences of magneto-optical effects (MOEs) in Ni–$Dy_{1-x}Ni_x$ bi-layer films [13]. In the temperature range 80–300 K, a Dy layer containing a Ni-impurity concentration x less than 5 wt% was found to make a temperature independent contribution to the MOE which is approximately equal in magnitude to the MOE of a $Dy_{1-x}Ni_x$ single layer observed only below the Curie temperature

* Corresponding author.
E-mail address: ise@iph.krasn.ru (I. Edelman).

0921-4526/$ - see front matter © 2008 Elsevier B.V. All rights reserved.
doi:10.1016/j.physb.2008.04.018

$T_C \approx 90$ K. This behavior of the MOE with variations in temperature was ascribed to ferromagnetic ordering of Dy caused by two factors: Ni atoms distributed over the entire Dy layer thickness and the spin system of the adjacent transition-metal layer. As this phenomenon revealed opens up the possibilities for changing the magnetic state of the RE metal, an investigation was undertaken devoted to a deeper experimental study, including *in situ* observation of the surface magneto-optical Kerr effect (SMOKE), and to investigate possible mechanisms responsible for it.

2. Experimental

Films were deposited on glass substrates (thickness, 0.8 mm; optical quality; surface finish class, 13) at a temperature of 250 °C. Pre-vacuum was 1×10^{-6} Pa, operating vacuum 1×10^{-5} Pa. The sputtered materials were Ni (vacuum melting) and Dy (class DiM 1). The deposition rates for Ni and Dy were approximately equal to 0.05 and 2.00 Å s^{-1}, respectively. First, a Ni layer was deposited on the substrate. Then, Ni and Dy were sputtered simultaneously. Step-shaped film samples were prepared with the use of special screen. Three part films were obtained by this method under identical conditions: a Ni single-layer film, a $Dy_{1-x}Ni_x$ single-layer film, and a Ni–$Dy_{1-x}Ni_x$ bi-layer film. The same method was used for preparing of NiFe–$Dy_{1-x}(NiFe)_x$. The thickness of each layer in the bi-layer film was equal to the thickness of the corresponding single-layer film. The Ni (or $Ni_{80}Fe_{20}$) content in the Dy layer and the thickness of Ni layers were specified by the conditions of Ni sputtering. Several series of film samples were prepared with 50- to 120-Å-thick Ni layers. The thickness of the Dy layers was varied from 200 to 700 Å. Reverse order of layer deposition was applied also, i.e., Dy or Dy with impurity was deposited first. Taken from the vacuum chamber, samples were cut into three parts according to visual boundaries between them. For all samples, the content of each component was determined by X-ray fluorescence analysis.

The distribution of the components over the area and thickness of a sample was determined by Auger electron spectroscopy [14] (sensitivity, 0.3 at%). The Auger electron spectra of the sample surfaces were recorded on a Riber OPC-2 Auger cylindrical-mirror analyzer with a relative resolution of 0.2%. The secondary electron spectrum was excited by an electron beam with energy of 3 keV. The electron beam diameter was equal to 5 nm, and the electron beam current amounted to 100 nA. The high-voltage modulation of the analyzer used was 6.88 eV. For several samples, secondary ion mass spectrometry (SIMS) was used with a quadruple mass-spectrometer MIQ-256 (CAMECA). O_2^+ ions with energy of 10 eV were used as primary beam. From some samples, X-ray photoemission spectra (XPS) were obtained using the MAC-2 "RIBER" cylindrical mirror. For excitation of X-ray emission, Mg or Al anodes were used with line energy Mg Kα $h\nu = 1253.6$ eV or Al Kα $h\nu = 1486.6$ eV, respectively. The X-ray beam diameter was 6 mm, the source capacity was 300 W, and the resolving power of the analyzer was 0.5 eV over the whole energy range.

For a layer-by-layer analysis (Auger, SIMS, and XPS), ion sputtering was accomplished using an argon-ion beam with an energy of 3 keV at an ion-beam current of 600 nA and a rate of approximately 10 Å/min. Since the substrate was prepared from a non-conducting material (glass), it was impossible to obtain spectral data for the film–glass interface due to strong charging of the glass surface. During the layer-by-layer analysis, the Auger or SIMS signals of the elements (Dy, 155 eV; Ni, 848 eV; O, 512 eV; and C, 272 eV) were measured as function of the time of etching of the sample with an argon-ion beam. The correct analysis requires standards and, besides, liberation of the second electrons depends on the matrix material. However, taking into account the proportionality of the signal to the amount of an element, these methods allow to make some estimations.

In order to control the degree of oxidation of the Dy layers during the magneto-optical experiments, the electrical conductivity of samples was measured.

The magnetic state of the samples was studied predominantly with the magnetic circular dichroism (MCD) method, because, first, this method is very sensitive and, second, there is no contribution from substrates to the MCD. The MCD was measured over the spectral range 350–650 nm as the difference $\Delta D = D^+ - D^-$ between the optical densities of a sample for waves having right-handed and left-handed circular polarization with respect to the external magnetic field. The magnetic field was directed normal to the sample plane and its strength was 4.5 kOe. The measurements were performed with the use of modulation of a light wave on the polarization plane, which was described for the first time by Jasperson and Schnatterly [15]. The MCD was measured with an accuracy of $\pm 10^{-4}$. The samples were cooled in a nitrogen-gas flow cryostat over the temperature range 80–300 K, with the temperature being maintained accurate to within ± 1 K. At room temperature, the field dependence of the polar Kerr effect (PKE) was measured in magnetic fields of up to 14 kOe directed normal to the sample plane.

The in-plane Kerr effect was measured "*in situ*" using an original technique that is similar to the torque magnetometer. A helium–neon laser beam ($\lambda = 630$ nm) came through the window in the vacuum chamber to the surface of the deposited film. The angle of the light incidence was 45° and the electric vector **E** of the light wave oscillated in the incidence plane (p-polarization). The reflected light passed through another window, analyzer and reached a photomultiplier. The signal at the photomultiplier output was proportional to the angle α_K between the orientations of the vector **E** in the incident and the reflected beams. The angle α_K is proportional, in its turn, to the projection of the film magnetization on the plane of the light incidence. A magnetic field of a permanent magnet of about 400 Oe was rotated in the plane of the film. The signal was recorded as a function of the angle φ between the magnetic field direction and the plane of the light incidence. In the absence of magnetization in a film, the signal is zero. If α_K is due to the longitudinal Kerr effect only the maximal signal will be observed for magnetization parallel to the plane of the light incidence, and signal will be zero for the magnetization direction normal to the light incidence plane. Contributions of other effects like transverse Kerr effect or intensity effect make the picture more complicated but anyhow the occurrence of the Kerr signal can be considered as evidence for a ferromagnetic state of a film.

3. Experimental results

Auger and SIMS results showed that Ni (or Ni+Fe) was distributed uniformly over the entire thickness of the Dy layer in the cases when these metals were deposited simultaneously with Dy onto preliminary deposited Ni film. The Ni concentration inside the Dy layer was varied from 0.00 to 0.06. When Dy alone was deposited onto the Ni film, there was a rather sharp interface between the two layers. Several examples are shown in Figs. 1 and 2. It is impossible to neglect the oxygen peak in the Auger spectrum which is especially strong near the surface. The oxygen content can be estimated according to ratio between the oxygen and Dy peaks, (I_O/I_{Dy}). For the spectrum shown in Fig. 1 this ratio is about 2. A high oxygen content has been reported by most of the authors studying Dy. Even in the standard Dy sample presented in Ref. [16] a large oxygen content was detected and I_O/I_{Dy} was 0.6.

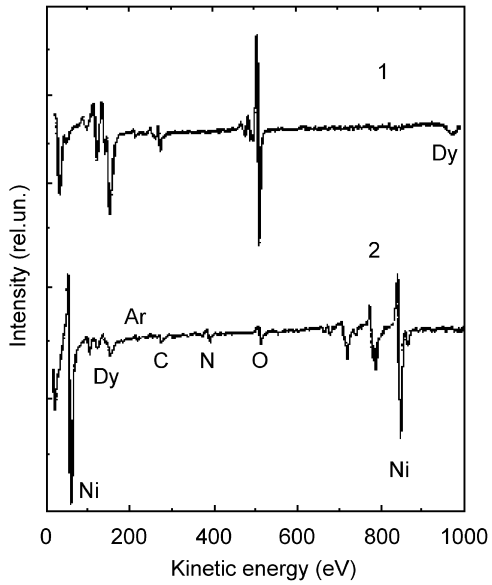

Fig. 1. AES of the bilayer film Dy(700 Å)–Ni(100 Å): (1) Dy layer; and (2) Ni layer.

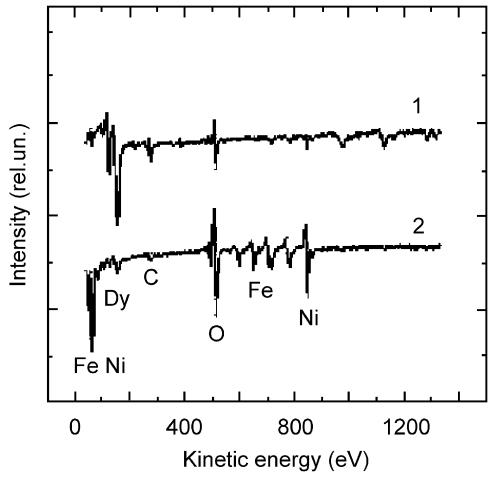

Fig. 2. AES of the bilayer film NiFe(50 Å)–$Dy_{0.94}(NiFe)_{0.06}$(500 Å): (1) $Dy_{0.94}NiFe_{0.06}$ layer; and (2) NiFe layer.

Fig. 3 demonstrates the dependence of the SIMS signal on the etching time for the sample NiFe–$Dy_{0.94}(NiFe)_{0.06}$. The curves 1 and 2 were obtained using suppression of the Ni and Fe signals with a negative voltage of 50 V and the Dy signal (curve 3) was suppressed by a negative voltage of 20 V. An increase of the Dy signal in the beginning and end parts of the curve is due to the increase of the secondary ions efficiency because of the larger part of oxidized Dy at the film surface and at the boundary with the NiFe layer. All over the central part of the Dy layer, Ni and Fe are distributed approximately homogeneously in accordance with the Auger-spectroscopy data.

As concerns oxygen, besides of its total amount, the state—free or bound—is of importance. As seen from the X-ray photoemission spectrum (Fig. 4), the oxygen signal consists of two components O1s (1) and O1s (2) corresponding, evidently, to two different oxygen states with larger and lower bonding energy. A similar picture was observed earlier, for example, a double maximum was observed in the O1s oxygen spectrum of La_2O_3–P_2O_5 glass [17]. The component positions depended on the relative amount of La and P in the glass. In our case, in the near-surface film region, the higher energy component O1s (1) prevails. Its intensity decreases sharply when deeper into the film, and at a depth of about 4 nm the component O1s (2) becomes prevailing. The corresponding bonding energy is close to the O1s bonding energy of 528–533 eV in the most of the oxide compounds [18]. At larger depth, the O1s (2) component intensity decreases again. One can suppose the O1s (1) peak to be due to oxygen molecules adsorbed at the film surface. The Os1 (2) component corresponds then to the formation of Dy oxide of which the amount diminishes with increasing depth, in accordance with the total oxygen decrease. So, Auger, SIMS and XPS allow to make conclusions about the metallic state of the largest part of Dy films. This conclusion was confirmed by the low electric resistance value ($\sim 5 \times 10^{-5}\,\Omega\,cm$) and the high optical absorption ($\sim 10^{-5}\,cm^{-1}$).

The spectral dependences of the MCD of $Dy_{0.95}Ni_{0.05}$ and Ni films at 93 and 300 K are shown in Fig. 5 (curves 1 and 2, respectively). The MCD in Ni film has a negative sign; its spectral dependence is similar to that of the polar magneto-optical Kerr effect for the Ni single crystal measured by Buschow et al. [19]. At 93 K, the MCD of the $Dy_{0.95}Ni_{0.05}$ film is comparable in magnitude to the MCD of the Ni film but is opposite in sign in the region 420–700 nm where two broad overlapping maxima can be seen.

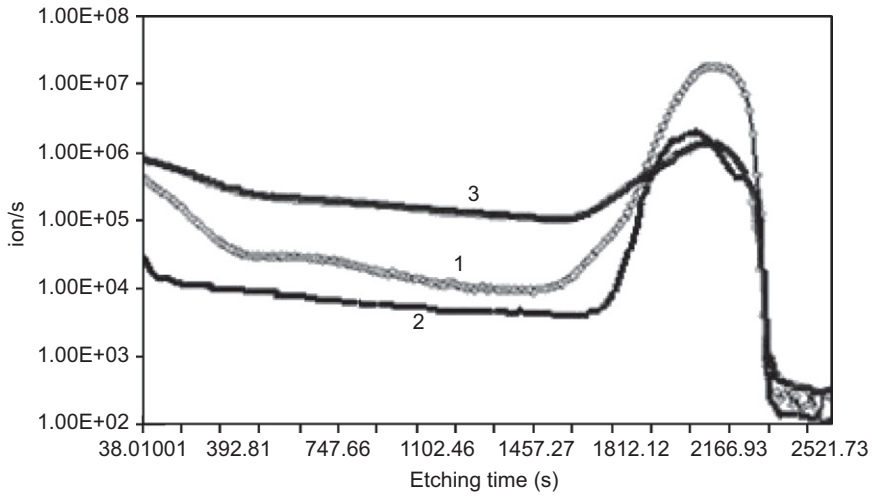

Fig. 3. SIMS of the bilayer film NiFe(67 Å)–$Dy_{0.94}(NiFe)_{0.06}$(620 Å) in dependence on etching time: 1, 2, 3—Ni, Fe, Dy, respectively. The Ni and Fe signals were suppressed with a negative voltage of 50 V and the Dy signal was suppressed by a negative voltage of 20 V.

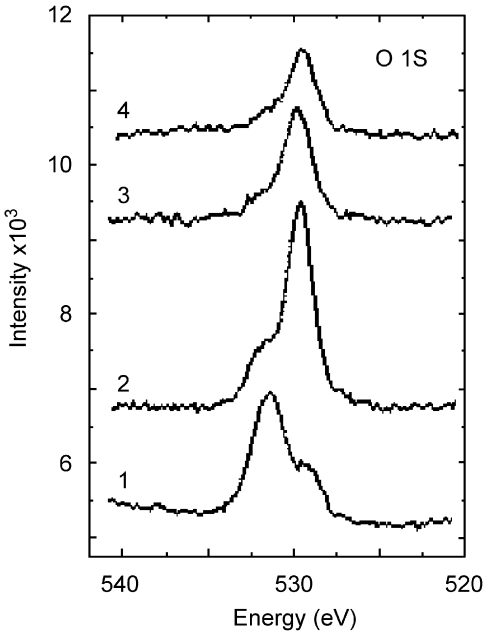

Fig. 4. XPES at different depths of $Dy_{0.94}(NiFe)_{0.06}$ film: (1) film surface; (2) 40 Å; (3) 300 Å; and (4) 400 Å.

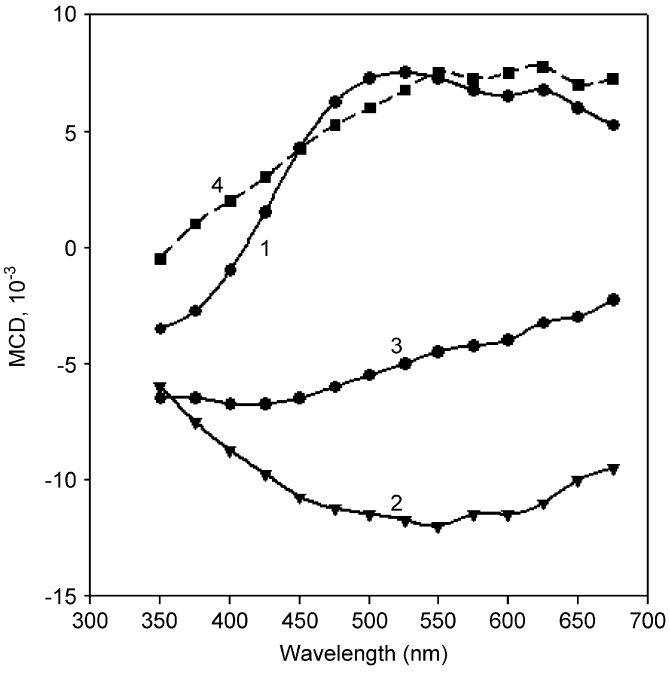

Fig. 5. MCD spectra of $Dy_{0.95}Ni_{0.05}$, Ni, Ni-$Dy_{0.95}Ni_{0.05}$ films (1, 2, and 3, respectively) and (4) the difference of curves 2 and 3. $T = 83$ K for curve 1 and $T = 300$ K for curves 2 and 3, $H = 4.5$ kOe.

In the same spectral range, Knyazev and Noskov [20] have observed a maximum in the spectrum of the off-diagonal component of the optical conductivity tensor σ_{xy} for a bulk Dy crystal. Near about 420 nm, the MCD reverses its sign. The MCD spectra for different Dy samples are similar. Small differences observed in the vicinity of the maximum can be associated with imperfection of the films. However, the point at which the MCD reverses sign remains the same for all the studied samples. As the measurement temperature was increased to 300 K, the MCD of the Dy film decreased by one order of magnitude (Fig. 6, curve 1) but remained of finite value. Besides, the transition to the

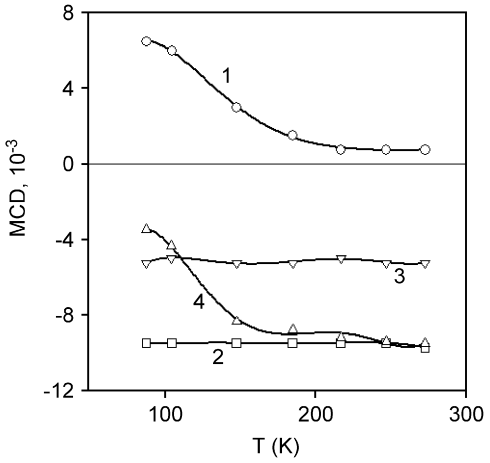

Fig. 6. MCD temperature dependences for the films: (1) $Dy_{0,95}Ni_{0,05}$ (620 Å); (2) Ni (70 Å); (3) Ni(70 Å)–$Dy_{0.95}Ni_{0.05}$(620 Å); and (4) sum of the curves 1 and 2. $\lambda = 550$ nm, $H = 4.5$ kOe.

ferromagnetic state occurs in a much wider temperature interval than in a high-quality Dy single crystal [3]. The same behavior was observed for the magnetization of fine-grained Dy samples measured at room- and liquid-nitrogen temperature [4]. Since the MCD is a linear function of the magnetization, there is a one-to-one correspondence between the temperature dependences of the magnetization and MCD, and one can ascribe the observed behavior of the MCD with temperature to size effects just as it was suggested in Ref. [4] for the magnetization of fine-grained Dy samples.

Comparison of the results obtained with the results in Refs. [4,20] confirms that the films investigated are of metal Dy, indeed. Dy oxides can present in the films in some low proportion but they give no contribution to the MCD; specially performed total oxidation of the films leads to disappearance of the MCD.

For Ni films with a thickness of about 80 Å or larger, the behavior of the MCD with temperature (Fig. 6, curve 2) corresponds to the magnetization behavior of bulk Ni samples in the same temperature interval (see Fig. 18.1 in Ref. [21]). For the $Dy_{1-x}Ni_x$ single layers with the x values used, the MCD spectral and temperature dependences coincide practically with that for Dy films. So, Ni impurities in such concentrations do not affect significantly the magnetic properties of a Dy film. The MCD temperature dependence of the Ni–Dy bilayer film is the simple sum of two curves: the MCD temperature dependence of a Ni film and temperature dependence of a Dy film (Fig. 6, curve 4). So, the contact with the Ni film does not affect the magnetic properties of the Dy film also. But when the $Dy_{1-x}Ni_x$ layer is sputtered onto the Ni layer, the situation becomes completely different: for x exceeding the threshold value ~0.05, the character of the temperature dependence of the MCD is similar to that for a Ni film but the magnitude of the MCD is close to the sum of the MCD magnitudes exhibited by Ni and Dy single layers at $T < T_C$ (Fig. 6. curve 3). Thus, the temperature dependence of the MCD is unusual in this case. One might suppose that Dy has an effect on the MCD of Ni and decreases its magnitude. However, we carried out an experiment on Dy oxidation and found out that complete oxidation of the Dy layer (a reference Dy single layer was oxidized to Dy_2O_3), under the condition that the Ni layer remains in the metallic state, causes the MCD magnitude to recover to that of a reference Ni single layer. The considerable contribution from the $Dy_{1-x}Ni_x$ layer to the overall MCD of the bi-layer film may be due to ferromagnetic ordering of this layer at temperatures far exceeding T_C of the corresponding single layer. The sign of this contribution is the same as that of the MCD of Dy at $T < T_C$. Based

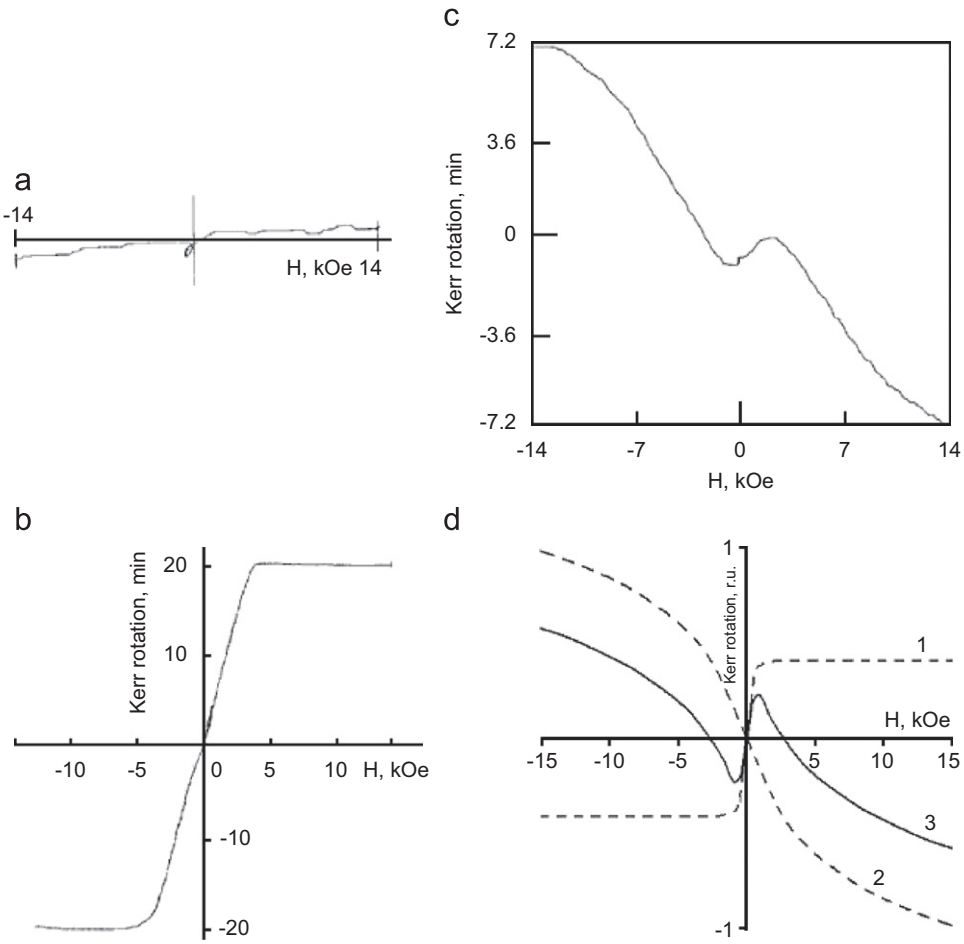

Fig. 7. Magnetic-field dependence of the PKE for light reflected from the Dy film (a), from the Ni film (b), and from the $Dy_{0.95}Ni_{0.05}$ layer in the bilayer film Ni–$Dy_{0.95}Ni_{0.05}$ (c). (d) Schematic presentation of curve c as the sum of two curves with different weight. $T = 300$ K. Wave length 670 nm.

on this fact, we can assume that the magnetic moments of Ni and $Dy_{1-x}Ni_x$ layers are parallel to each other.

In contrast to the MCD, which is the integral effect exhibited by both layers of a bi-layer film, measurements of the PKE and LKE characterize each of these layers separately. When light is reflected by the Dy or $Dy_{1-x}Ni_x$ film, Kerr effects are not observed at room temperature. The situation is shown in Fig. 7a for the $Dy_{0.95}Ni_{0.05}$ film. In the case of the Ni film the magnetic-field dependence of the PKE (Fig. 7b) is typical for a film with in-plane magnetic anisotropy. As it is seen in Fig. 7c, the PKE is observed at room temperature when light is reflected by the $Dy_{0.95}Ni_{0.05}$ layer in the bi-layer film. The PKE sign is opposite to that of the Ni film and magnetic-field dependence of the PKE is quite different compared to the Ni film. While the saturated magnetic field H_s for the Ni film is of about 4.5 kOe, in accordance with Ni spontaneous-magnetization value ($I_s = 480$ Gs), in the case of light reflection from the $Dy_{0.95}Ni_{0.05}$ layer in the bi-layer film, magnetic saturation is not reached up to highest value of 14 kOe of the magnetic field used. The S-shape feature of the curve of the magnetic-field dependence of the PKE near zero magnetic field can be easily explained by the contribution of the PKE of the bottom Ni layer of the positive sign owing to the light reflection at the boundary between the two layers as is shown schematically in Fig. 7d. The PKE data cited above leave no doubts that the $Dy_{1-x}Ni_x$ layers in the bi-layer films considered have their own contribution to the MOEs of the bi-layer films at room temperature and, hence, these layers possess a spontaneous magnetic moment at room temperature. The H_s value in this case exceeds essentially 14 kOe which allows to think about a magnetization value close to that of Dy bulk samples observed generally at low temperatures.

Now we consider the results of *in situ* room-temperature LKE measurements that are of importance because of the low oxidation of the samples. Curve 1 in Fig. 8 shows the Kerr signal of the Ni film via the direction of the in-plane magnetic field with respect to the plane of the light incidence onto the film surface. Periodical changes of the LKE value reflect changes of the film magnetization projection on the light-incidence plane. Some deviations of the LKE curve with strong periodicity will be discussed elsewhere. For the Dy or $Dy_{1-x}Ni_x$ films, or the Dy-layer deposited onto the Ni layer, there is no LKE signal. But, when a $Dy_{1-x}Ni_x$ layer is deposited onto the Ni layer a LKE signal appears of the opposite sign compared to the LKE sign of the Ni film. Curve 2 in Fig. 8 shows the LKE signal for the $Dy_{0.95}Ni_{0.05}$ layer on Ni. The opposite sign of the $Dy_{0.95}Ni_{0.05}$ LKE compared to the Ni LKE agrees with the opposite PKE signs for these two cases. The stronger angle lag of LKE in this case compared to that for the Ni film evidences a higher $Dy_{0.95}Ni_{0.05}$ layer anisotropy than the anisotropy of the Ni layer. So, *in situ* data confirm the magnetic-moment appearance in the Dy layer doped with a low concentration of Ni impurities when this layer is in atomic contact with the continuous Ni layer.

Summing up the results of magneto-optical experiments, one can conclude that the appearance of MOEs in the films investigated at temperatures exceeding essentially Curie temperature of the bulk Dy can be due to the appearance of magnetic order in the $Dy_{1-x}Ni_x$ layer under its condition of direct contact

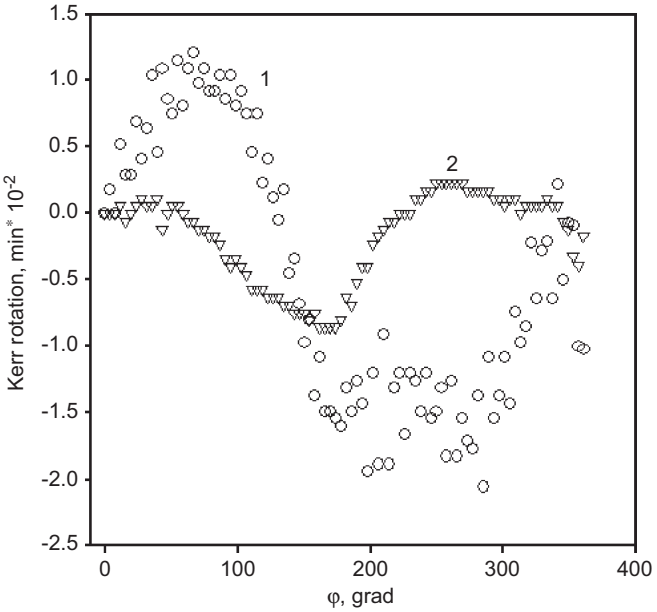

Fig. 8. Room-temperature LKE (*in situ*) in dependence on the direction of the in-plane magnetic field relative to the plane of the light incidence onto the film surface: (1) signal of the Ni film; and (2) signal of the $Dy_{0.95}Ni_{0.05}$ layer on Ni.

with the continuous Ni layer. The magnetic moment of $Dy_{1-x}Ni_x$ is parallel to the Ni layer moment and its value exceeds the Ni layer moment, at least, in four times. The critical Ni concentration in the Dy layer depends on the Dy-layer thickness and is about $x = 0.05$ for a thickness of about 50 nm.

4. Discussion

Comparison of the magneto-optical data with the Auger-spectroscopy results shows that incorporation of Ni or NiFe into a Dy layer changes essentially its magnetic properties. One can assume the changes observed to be due to an interface layer with high concentration of Ni or NiFe. However, in this case there would be no proportionality between the MCD value and the thickness of the $Dy_{1-x}Ni_x$ layer which is observed in the experiment. The supposition is possible also that the Ni concentration may be high enough for formation of Ni nanoparticles in the Dy layer, but in this case similar behavior should be observed in the $Dy_{1-x}Ni_x$ layers independently of the existence of an adjusting Ni layer. The observed field dependences of the PKE and LKE are inconsistent with the assumption that the magnetic ordering of the $Dy_{1-x}Ni_x$ layer is magnetostatic in nature. Moreover, if the Dy layer would be simply magnetized by the magnetic field of the Ni layer, this would also have occurred in the Ni–Dy bilayer film, which was not the case. It also does not seem likely that the magnetic state of the $Dy_{1-x}Ni_x$ layer in bilayer films changes due to magnetostriction via the mechanism proposed in Ref. [22], because these films are not epitaxial. If the change in the structural parameters causing the magnetic ordering had been due to incorporated Ni atoms, an analogous effect would also have been observed in the $Dy_{1-x}Ni_x$ single layers, which was not the case. Thus, the unusual behavior of the Dy magnetic system is associated with the simultaneous influence of two factors: the contact with a 3d metal layer and inclusion of 3d elements distributed approximately homogeneously over the whole Dy layer. Each of these factors has separately no essential influence on the magnetic state of the Dy layer.

As is known, the magnetic structure of heavy RE metals (including Dy) is mainly determined by the exchange interaction of the conduction electrons with 4f electrons [21]. The indirect exchange interaction leads to ordering of large 4f magnetic moments. The conduction electrons are characterized by the band exchange interaction I of which the value is not large enough to satisfy the Stoner criterion $IN(\varepsilon_F) > 1$, where $N(\varepsilon_F)$ is the density

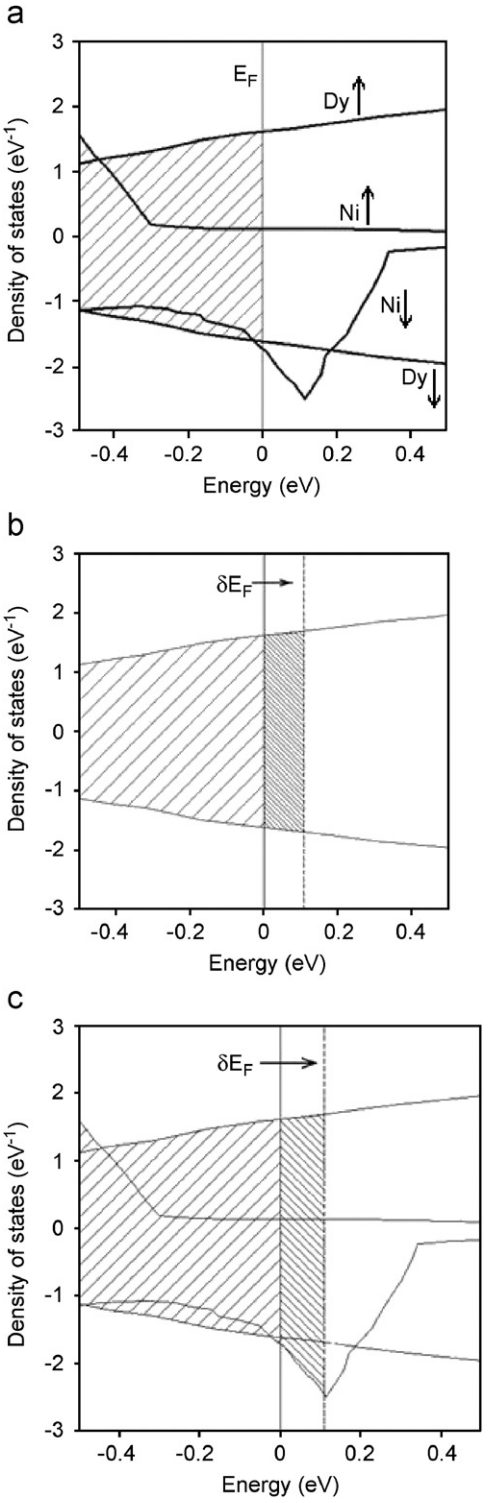

Fig. 9. Schematic diagram of the density of states: (a) alloy $Dy_{1-x}Ni_x$; (b) bilayer film Ni–Dy, and (c) bilayer film Ni–$Dy_{1-x}Ni_x$. The shift in the Fermi level caused by the penetration of electrons from the Ni layer is indicated.

of states at the Fermi level. Therefore, the conduction-electron spins are not ordered and behave as a paramagnetic system in the effective magnetic field of the localized 4f moments. Incorporation of Ni atoms into a Dy layer causes changes in the system of conduction electrons. We propose the following model for these changes. Like in the virtual-crystal model, we can write the density of states of the $Dy_{1-x}Ni_x$ alloy in the form

$$N(E) = (1-x)N_{Dy}(E) + xN_{Ni}(E).$$

The density of states of Dy near the Fermi level has no peculiarities and is dominated by the 5d electrons with a small admixture of 6s and 6p electrons [23,24]. In Ni, there is a narrow filled peak of "spin-up" electronic states and a narrow unfilled peak of "spin-down" electronic states [25]. The density of states of the alloy is shown schematically in Fig. 9, where the Fermi levels of both alloy components are assumed to be equal. Similar to bulk Ni, in the $Dy_{1-x}Ni_x$ alloy layer, in the model considered, there is a narrow filled peak with spin up and empty peak with spin down situated right above ε_F. In the case of the bi-layer Dy–Ni film the electron concentration in the Dy layer increases owing to the contact with the Ni layer and Ni atoms penetrate at some depth into the Dy layer and, consequently, the Fermi level shifts (Fig. 9b). However, because of the absence of peculiarities in the Dy density of states at the scale of about 0.1 eV in the vicinity of ε_F, this shift does not change $N(\varepsilon_F)$ significantly. So, in both cases, the dimensionless parameter of the band exchange $IN(\varepsilon_F)$ changes only slightly compared to that in Dy.

When we deal both with contact of Dy layer with the Ni layer (i.e., the shift of chemical potential) and with Ni atoms that are introduced into the Dy layer which leads to the formation of a narrow peak in the density of states near the Fermi level, then the chemical potential may coincide with the peak in $N\downarrow(\varepsilon_F)$ at a certain concentration x_c (Fig. 9c). As a result the Stoner factor increases. The ferromagnetism observed at room temperature in the $Dy_{1-x}Ni_x$ layer on the Ni substrate can be considered as a consequence of reaching the Stoner criterion $IN(\varepsilon_F)>1$ which leads to the magnetic ordering of the conduction-electron moments along the 4f moments. So, Ni as a component of an alloy contributes the density of states with the peculiarity near the Fermi surface and the penetration of Ni atoms from the adjusting Ni layer leads to the occupation of the states near this peculiarity and to a change of the magnetic properties of the $Dy_{1-x}Ni_x$ layer.

The suggested mechanism of magnetic ordering (through the conduction electrons) should result in a different character of the temperature dependence of the magnetization and the MOEs of the $Dy_{1-x}Ni_x$ layer in comparison with the magnetization due to the ordering of the 4f moments in Dy at $T<T_C$. Such a phenomenon is observed really in the case considered as is seen from experiments.

Acknowledgments

The work was supported partly by the Integration Project of SB RAS (# 3.5), Program "Spintronics" of the Department of Physical Sciences of RAS, and RFBR Grant no. 07-03-00320.

References

[1] K.P. Belov, Rare Earth Magnetics and Their Application, Science, Moscow, 1980.
[2] S.A. Nikitin, Magnetic Properties of Rare Earth Metals and Their Compounds, Moscow State University Publishing House, Moscow, 1989.
[3] A.S. Chernyshov, A.O. Tsokol, A.M. Tishin, et al., Phys. Rev. B 71 (2005) 184410.
[4] Ch.Ja. Mulyukov, G.F. Korznikova, S.A. Nikitin, Fiz. Tverd. Tela 37 (1995) 2481.
[5] Y. Ufuktepe, J. Phys.: Condens. Matter 5 (1993) L213.
[6] Z.S. Shan, D.J. Sellmyer, S.S. Jaswal, et al., Phys. Rev. B 42 (1990) 10446.
[7] Z.S. Shan, D.D.J. Sellmyer, Phys. Rev. B 42 (1990) 10433.
[8] Y. Kamiguchi, Y. Hayakawa, H. Fujimori, Appl. Phys. Lett. 55 (1989) 1918.
[9] A.L. Dantas, R.E. Camley, A.S. Carriço, Phys. Rev. B 75 (2007) 094436.
[10] A. Tamion, J. Juraszek, C. Bordel, J. Magn. Magn. Mater. 313 (2007) 306.
[11] K. Mibu, N. Hosoito, T. Shinjo, J. Magn. Magn. Mater. 126 (1993) 343.
[12] B. Scholz, R.A. Braud, W. Kenne, Phys. Rev. B 50 (1994) 2537.
[13] I.S. Edelman, V.V. Markov, S.G. Ovchinnikov, et al., Fiz. Tverd. Tela 45 (2003) 1423.
[14] L.E. Davis, N.C. MacDonald, P.W. Palmberg, et al., Handbook of Auger Electron Spectroscopy, second ed, Physical Electronics Industries Inc., Eden Prarie, MN, 1976.
[15] S.N. Jasperson, S.E. Schnatterly, Rev. Sci. Instrum. 40 (6) (1969) 6761.
[16] W. Koehler, E. Wollen, Phys. Rev. 92 (1953) 1380.
[17] T. Homma, Y. Benino, F. Fujivara, T. Komatsu, J. Appl. Phys. 91 (2002) 2942.
[18] T.L. Barr, Modern ESCA, The Principles and Practice of X-ray Photo-electronic Spectroscopy, CRS Press, Boca Raton, FL, USA, 1994.
[19] K.H.G. Buschow, P.G. van Engen, R. Jongebreur, J. Magn. Magn. Mater. 38 (1983) 1.
[20] Yu.V. Knjazev, M.M. Noskov, Fiz. Met. Metalloved. 30 (1970) 214.
[21] S.V. Vonsovsky, Magnetizm, Nauka, Moscow, 1971.
[22] C. Carbone, R. Rochov, L. Braicovich, et al., Phys. Rev. B 41 (1990) 3866.
[23] S.C. Keeton, T.L. Loucks, Phys. Rev. 168 (1968) 672.
[24] W. Schneider, S.L. Molodtsov, M. Richter, et al., Phys. Rev. B 57 (1998) 14930.
[25] A.I. Lichtenstein, M.I. Katsnelson, Phys. Rev. Lett. 87 (2001) 67205.